Histol Histopathol (2016) 31: 1347-1356

http://www.hh.um.es

Histology and Histopathology

From Cell Biology to Tissue Engineering

Nestin+cells forming spheroids aggregates resembling tumorspheres in experimental ENU-induced gliomas

Alvaro García-Blanco[1], Susana Bulnes[2], Iñigo Pomposo[3,4], Alex Carrasco[3,4] and José Vicente Lafuente[1,4,5]

[1]Laboratory for Clinical and Experimental Neuroscience (LaNCE), Department of Neuroscience, University of the Basque Country, [2]LaNCE, Department of Nursing I, University of the Basque Country, Leioa, [3]LaNCE, Department of Surgery, University of the Basque Country and Neurosurgery Department, Cruces University Hospital, Bilbao, [4]Group Nanoneurosurgery, Institut of Health Research Biocruces, Barakaldo, Spain and [5]Faculty of Health Science, Universidad Autónoma de Chile, Santiago de Chile, Chile

Summary. Nestin+cells from spheroid aggregates display typical histopathological features compatible with cell stemness. Nestin and CD133+cells found in glioblastomas, distributed frequently around aberrant vessels, are considered as potential cancer stem cells. They are possible targets for antitumoral therapy because they lead the tumorigenesis, invasiveness and angiogenesis. However, little is known about their role and presence in low-grade gliomas. The aim of this work is to localize and characterize the distribution of these cells inside tumors during the development of experimental endogenous glioma.

For this study, a single dose of Ethyl-nitrosourea was injected into pregnant rats. Double immunofluorescences were performed in order to identify stem-like and differentiated cells.

Low-grade gliomas display Nestin+cells distributed throughout the tumor. More malignant gliomas show, in addition to that, a perivascular location with some Nestin+cells co-expressing CD133 or VEGF, and the intratumoral spheroid aggregates of Nestin/CD133+ cells. These structures are encapsulated by well-differentiated VEGF/GFAP+cells. Spheroid aggregates increase in size in the most malignant stages.

Spheroid aggregates have morphological and phenotypic similarities to *in vitro* neurospheres and could be an *in vivo* analogue of them. These arrangements could be a reservoir of undifferentiated cells formed to escape adverse microenvironments.

Key words: Stem cells, Nestin, ENU, Glioma

Offprint requests to: Álvaro García, Neuroscience Department, Faculty of Medicine and Odontology, Barrio Sarriena, CP:48940 Leioa. e-mail: algarblandom@gmail.com

DOI: 10.14670/HH-11-763

Introduction

Nestin belongs to the group of intermediate filament proteins, ubiquitously distributed in several cell types (Morrison and Kimble, 2006). It is produced and expressed, among others, in stem cells of the mammalian CNS during development, being present in the early stages of neurogenesis in the subventricular zone (SVZ) (Fan et al., 2007), in human glioblastomas (Hadjipanayis and Van Meir, 2009) and is the leading molecule in this study.

Cancer stem cells (CSCs) show properties of adult stem cells, such as self-renewal, multilineage differentiation or asymmetric division (Clarke et al., 2006; Jang et al., 2006). The plasticity model of carcinogenesis (Dell'Albani, 2008) explains the glioma development throughout CSC growth, with the tumoral microenvironment acting as the determinant of the cell stem status (Messam et al., 2000). A variety of markers are usually used for the identification of CSCs (CD133, Nestin, Osteopontin, Notch-1 or Sox-2) (Singh et al., 2004; Arai et al., 2012), but none of these are specific for cancer stem cells.

CD133 was one of the first reported markers for cancer stem cells. It is a transmembrane glycoprotein (Jang et al., 2006) present in neural stem cells (Morrison and Kimble, 2006), ubiquitous in many tumoral stem cells and very useful as stemness marker, and it is

expressed by cells around the tumor vasculature (Kronenberg et al., 2003; Christensen et al., 2008; Grosse-Gehling et al., 2013). CSCs have been previously observed around tumoral vasculature, inside the perivascular niche (Christensen et al., 2008).

Because of the lack of specific markers for CSCs, the gold standard to identify them is the *in vitro* growth (Jensen and Parmar, 2006), followed by transplantation assay to assess their tumorigenicity, self-renewal, asymmetric division and sphere formation. These consist of globular arrangements of differentiated and undifferentiated cells with a rich extra-cellular matrix surrounding them (Pastrana et al., 2011).

For the present study, we have used the prenatal N-Ethyl-N-nitrosourea (ENU) model. In this model a single dose of ENU administered to pregnant rats induces neoplasias in the offspring (Adey et al., 2000; Bulnes-Sesma et al., 2006). ENU-gliomas provide a close model to human pathology, since the endogenous tumors are obtained subsequently to the action of an alkylating agent. These tumors replicate the growth curve of human ones and the model allows the study of the transition between low and high-grade gliomas (Gondo et al., 2010; Doblas et al., 2012). In recent years, the ENU model has been used for several studies, among them mutagenesis studies in mice (Gondo et al., 2010).

The aim of the present study is to identify and localize Nestin positive cells in an endogenous model of gliomas, from early to advanced stages, reporting their distribution in different tumoral areas and their co-expression with other stemness markers as well as their participation in cell clusters.

Materials and methods

Ten Sprague-Dawley rats were intraperitoneally injected with a single dose of ENU (80 mg/kg.b.w, 1% in PBS 0.1 M) at 15th day of pregnancy. 70 Offspring rats between 6-10 months old were sacrificed when they displayed health deficits. Rats were anesthetized and transcardially perfused with 0.9% saline following 4% paraformaldehyde in PBS 0.1 M (pH 7.4). Brains were immersed in the same solution at 4°C overnight and dissected in coronal sections. Some were cryopreserved in 30% sucrose and cut with a cryotome into 40 µm sections, others were embedded in paraffin blocks and cut into 4 µm sections.

Haematoxylin-eosin staining was carried out on paraffin sections, reporting histological features such as cellular proliferation, anaplasia, necrosis, haemorrhages, microvascular proliferation or glomeruloid-like vessels.

Immunohistochemistry

Using ABC method (Elite ABC Kit, Vector Laboratories), immunohistochemical assay was carried out on paraffin slices against Nestin (1:200 ref sc-33677, Santa Cruz). The reaction product was developed by 3.3-diamino-benzidine (Ref. 8001, Sigma-Aldrich) and H_2O_2 (0.01%).

Cryotome sections were used for double indirect immunofluorescence. The sections were incubated overnight at 4°C in a mix of Nestin (1:400 ref. sc-21247, Santa Cruz) and one of the following primary antibodies: VEGF (1:200 ref. sc-152, Santa Cruz), GFAP (1:400 ref. sc-6170, Santa Cruz), CD133 (1:100 ref. ab-16518, Abcam), GluT-1 (1:200 ref. 07-1401, Millipore).

The next day, tissues were incubated in a mix of secondary antibodies: FITC-conjugated anti-mouse IgG (1:400 ref. F-9137, Sigma-Aldrich) and TRITC-conjugated anti-rabbit IgG (1:400 ref. T-6778, Sigma-Aldrich). Finally, sections were incubated in Hoechst 33258 (Sigma-Aldrich) 5μg/ml in PBS 0.1M during 10 minutes.

Lectin histochemistry

Lectin histochemistry was performed on free-floating cryotome slices. The tissue was incubated overnight at 4°C with FITC-conjugated *Lectin lycopersycum* (1:100 ref. L0401, Sigma). Cases were double stained with CD133 as previously described.

Negative controls, omitting primary antibodies, were also included in each staining run. All immunofluorescence images were acquired with an Olympus Fluoview FV500 confocal microscope using sequential acquisition to avoid overlapping of fluorescent emission spectra. Images have been treated with *FV10-ASW 1.6 Viewer* and *Adobe Creative Suite 4*.

Quantification

Nestin positivity index was calculated counting 400 tumor cells at high magnification (×400), with a reticule of 62,500 µm^2, from the most representative areas of tumors, and the percentage of Nestin+cells was reported. Only positive cells not in contact with vessels and localized individually were counted, not considering aggregation of cells.

The number of intratumoral aggregates in the same cases was also counted, considering only the aggregations of 6 or more Nestin+cells with small cytoplasm and without prolongations. The area of these aggregates was calculated using *Image J* software.

Quantitative evaluation was performed by the same researcher to avoid inter-observer variability.

Statistical analysis

All the statistical analyses were performed using *GraphPad Prism 5.00*. An unpaired t-test was used to analyze differences among the means of the Nestin positivity index. Data are described as mean±SEM, p values less than 0.05 are considered statistically significant.

Ethical standards

Animal experiments were performed in accordance with Spanish RD1201/2005, European Directive

2003/65/EC and European Recommendation 2007/526/EC.

Results

104 gliomas coming from 70 rats were considered for the present study.

On the basis of previous studies (Bulnes and Lafuente, 2007) ENU-gliomas were divided into three stages (corresponding to malignancy features like: tumor size, cell proliferation, nuclear anaplasia, microvascular changes, haemorrhages, cysts or necrosis).

In the initial stage (or stage I), 37 small-middle size cell proliferations were found shaping well-delimited tumors, mainly associated with subcortical white matter (Fig. 1a,b). Histopathologically, they are composed of isomorphic round cells with well-defined regular nuclei and a clear halo around them. They also have fine microvessels constituting a network mimicking normal brain microvasculature. This stage corresponds to classic oligondendroglioma (WHO, grade II). In this stage, some Nestin+cells with large cytoplasm and large prolongations were distributed throughout the tumoral mass (Fig. 1c).

30 tumors were grouped in the intermediate stage (or stage II). These tumors are well-defined (Fig. 1d,e), neuropathologically display mild vessel aberration (dilated and tortuous vessels) and some other histopathological features like anaplasia with atypical mitosis or sporadic nuclear polymorphism. This stage

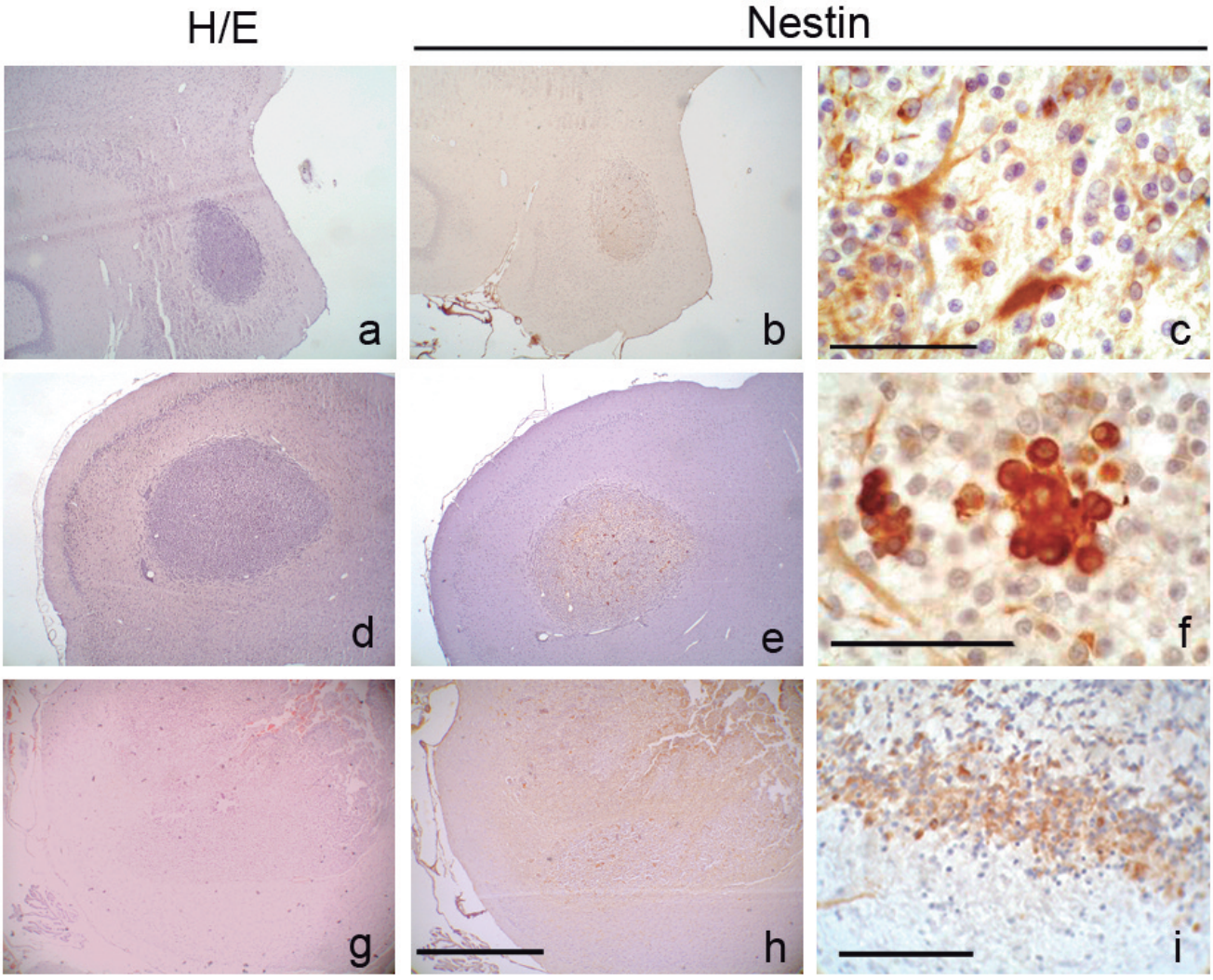

Fig. 1. Distribution of Nestin+cells in various ENU-gliomas. Stage I **(a, b, c)** some Nestin+cells are distributed randomly inside the tumor. Stage II **(d, e, f)** numerous aggregations of small round Nestin+cells are to be observed. Stage III **(g, h, i)** Scattered Nestin+cells are distributed inside the pseudopallisade around necrosis. **(i)**. Scale bars: a, b, d, e, g, h, 2.5 mm; c, f, i, 10 µm.

would represent anaplastic oligodendroglioma (WHO grade III). Nestin+cells with round and scarce cytoplasm and hyperchromatic nuclei form groups that we have called "spheroid aggregates" (SA) (Fig. 1f).

37 tumors were classified in the most malignant or advanced stage (or stage III), characterized by being huge tumors (≥25% of coronal slices) (Fig. 1g,h) with macro-haemorrhages, prominent microvascular proliferation and abnormalities like glomeruloid vessels, macrocysts and necrosis with occasional pseudo-palisading. This stage would be equivalent to Glioblastoma Multiforme (WHO grade IV). Inside the rich cellularity of pseudo-palisades around necrotic foci, it is very frequent to find a scattering of Nestin+cells (Fig. 1i). In addition, intense Nestin+cells in this stage are frequently localized inside the tumor, being part either of spheroid aggregates or being attached to the vascular wall (Fig. 2). On the border of the tumors, there are heterogeneously distributed big and well-differentiated cells positive for Nestin, which resemble hypertrophic astrocytes.

CD133+cells can only be observed in tumoral stages II and III and they are always small round cells mildly stained inside spheroid aggregates (Fig. 3c) or sitting close to vessels (Fig. 4g,h,l,m).

Spheroid aggregates

Spheroid aggregates are characterized for being groups of at least six positive cells for Nestin and/or CD133. These cells have a characteristic morphology, with a round form, scarce cytoplasm and dense nuclear chromatin, resembling the morphological features of stem cells. Aggregates can be found heterogeneously distributed within the tumor in all the stages of glioma development but they appear predominantly in the intermediate and advanced stages (II and III), tending to form sphere-like shapes (Fig. 1f). Some cells inside the

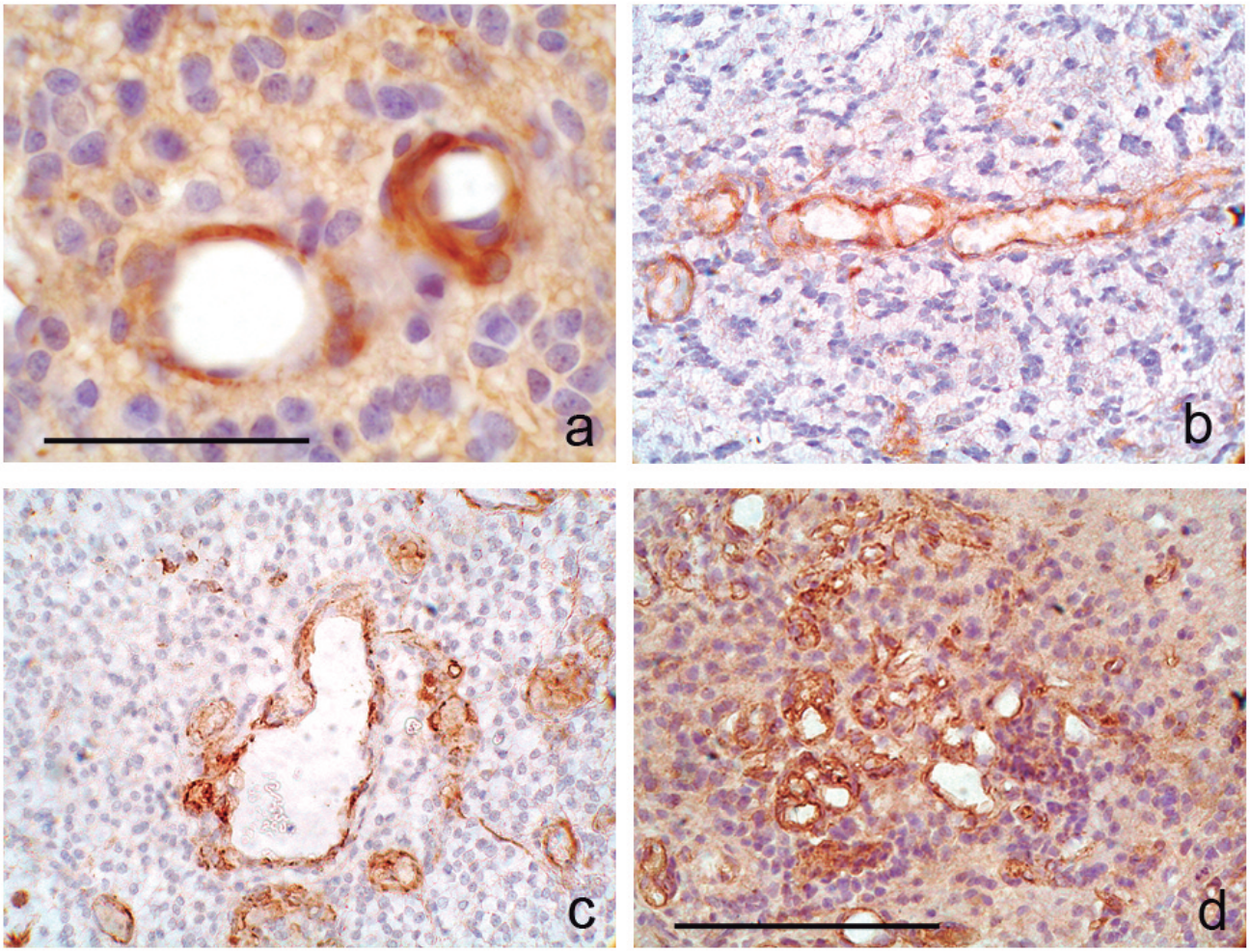

Fig. 2. Distribution of Nestin positivity in endothelium of microvessels and in cells around them from different stages. Stage I **(a)**, stage II **(b, c)**, stage III **(d)** showing glomeruloid vessels. Scale bars: a, 10 µm; b-d, 25 µm

aggregates co-express Nestin and CD133 (Fig. 3c, arrowhead).

Aggregates are usually surrounded by GFAP+cells, which seem to be "encapsulating" these cellular arrangements (Fig. 3b). Some cells either at the periphery of these formations, or inside them, co-express slightly VEGF and Nestin (Fig. 3a, arrow). These arrangements seem to include immunopositive

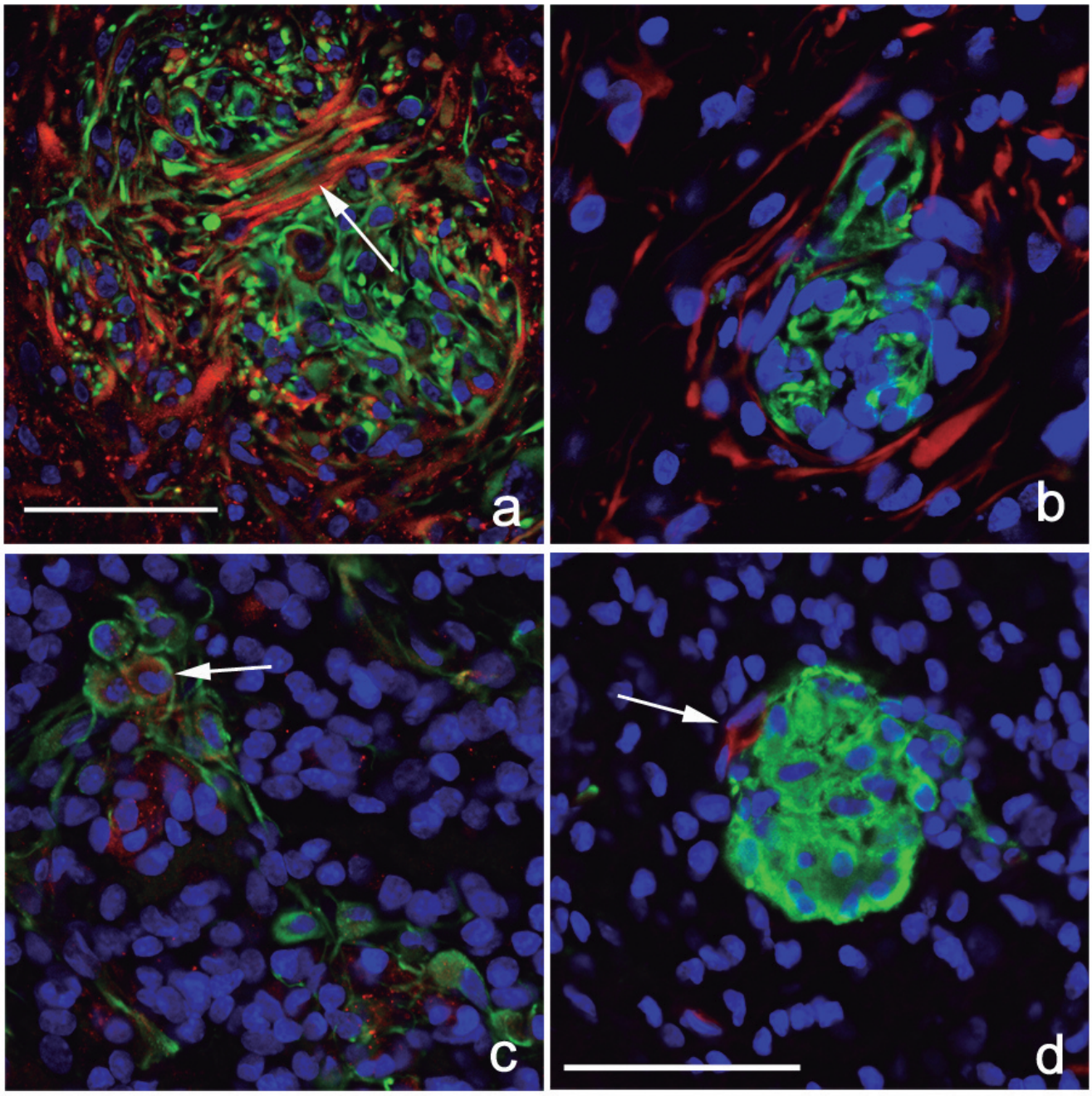

Fig. 3. Distribution of Nestin positivity in small spheroid aggregates and its relationship with other immunomarkers; Nestin is visible in green in the immunoflorescence and in red -VEGF **(a)**, -GFAP **(b)**, -CD133 **(c)** and -GluT-1 **(d)**. Pictures **a** and **d** correspond to stage III tumors, while **b** and **c** correspond to stage II. VEGF **(a)** is mainly localized around Nestin+cells and occasionally may be found co-localizing in some cellular prolongation. GFAP **(b)** is localized externally to the agreggate. CD133 **(c)** is found in the same cells showing a complementary pattern of immunostaining. Glut-1 **(d)** denotes the presence of a microvessel close to the spheroid aggreggate. Scale bars: 25 μm

microvessels for GluT-1 inside them (Fig. 3d, arrow).

Perivascular niche

To elucidate the distribution of Nestin/CD133+cells around vessels, it must be taken into account that Nestin also stains immature endothelial cells, as previously stated by Matsuda and collaborators (2013). Only using specific endothelial or BBB functional markers it is possible to differentiate what belongs to the microvasculature and what to the tumoral mass. Using GluT-1 as an early BBB marker and LEA as an endothelial marker, we found Nestin expression in tortuous vessels (Fig. 4a), co-expression with Glut-1 when vessels become dilated (Fig. 4f), and a complementary distribution in glomeruloids (Fig. 4k).

Tumoral Nestin+cells are to be found around all abnormal types of vessels (tortuous, dilated and glomeruloid ones) (Fig. 4b, g, l). In glomeruloids, Nestin+cells are located close to the vessel wall, frequently co-expressing CD133 (Fig. 4l). Using a specific endothelial marker like LEA, we could appreciate that some endothelial cells in glomeruloids also co-express CD133 (Fig. 4m). In other abnormal vessels, like tortuous and dilated ones, CD133+cells with a small round shape are close to the vascular endothelium stained with LEA (Fig. 4c,h).

In addition, co-expression of GFAP (Fig. 4d,i,n) and VEGF (Fig. 4e,j,o) with Nestin was only observed around dilated vessels (Fig. 4i,j), but GFAP and VEGF+cells appear mainly surrounding Nestin+cells.

Quantification of Nestin+cells and spheroid aggregates

The Nestin positivity index was calculated in 87 gliomas from 53 rats, 31 gliomas of stage I, 25 of stage II and 31 of stage III. An increase in Nestin expression during glioma progression was observed. In the initial stage I, Nestin positivity index is 5.26±0.60 (N=31), in the intermediate stage II is 10.25±0.91 (N=25) and 15.94±1.27 in the most advanced stage III (N=31). A statistically significant increase among all stages was obtained (stage I vs. II $p<0.0001$; stage II vs. III $p=0.01$; stage I vs. III $p<0.0001$) (Fig. 5a).

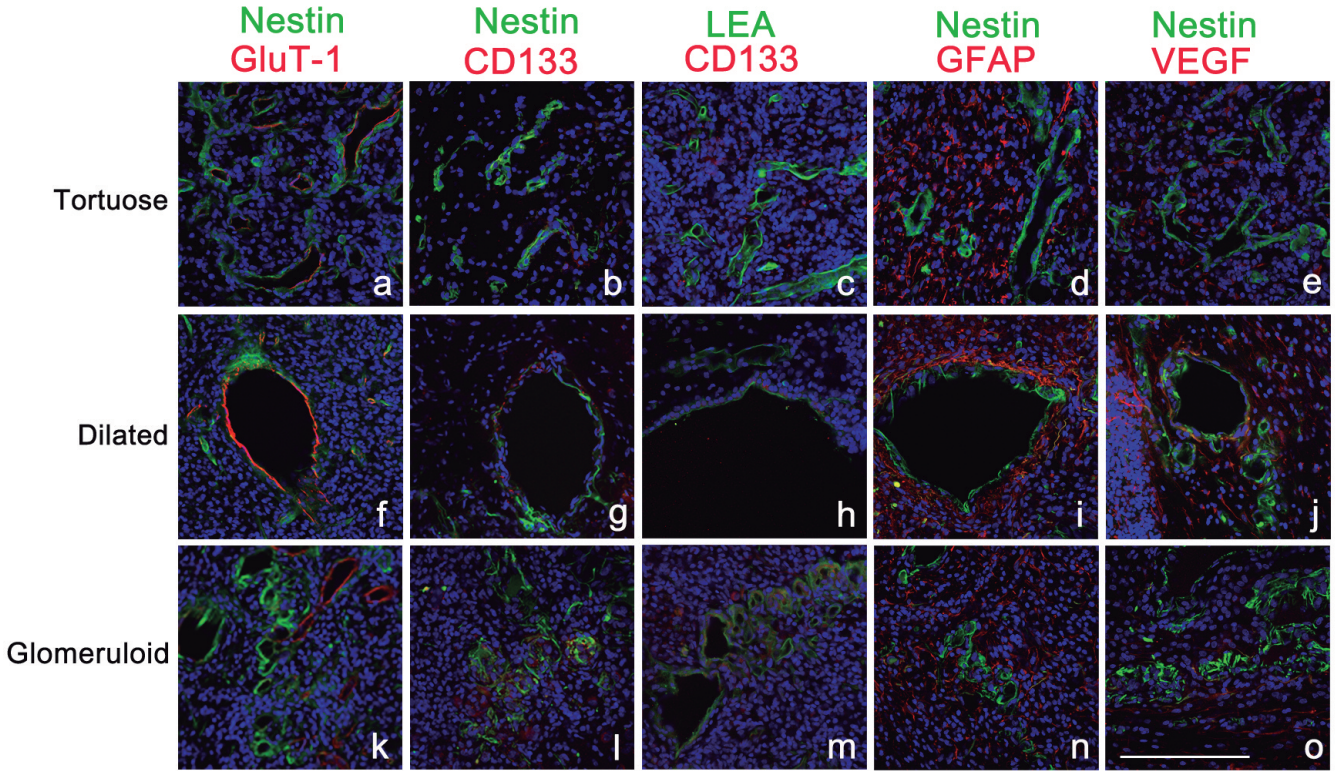

Fig. 4. Distribution of Nestin positivity (green) and other immunomarkers (red) regarding various types of microvessels. All slices are counterstained with Hoechst (blue). Nestin and Glut-1 respecting vessels **(a, f, k)** seem to stain in a complementary way, when coinciding, Glut-1 is always the most internal layer. There is co-expression of Nestin-CD133 (**b, g, l**) only in and around glomeruloid vessels. Some small round cells mildly positive for CD133 are scattered, distributed around different types of vessels stained by LEA (**c, h, m**). In dilated vessels **(h)**, CD133 is very close to the vessels wall, while in glomeruloid vessels both markers co-express on the vascular wall. GFAP+structures **(d, i, n)** frequently surround the Nestin positive ones, only occasionally in **(i)** and **(n)** is to be found some co-expression. VEGF positivity around vessels **(e, j, o)** is suspected to correspond with GFAP positive structures resembling astrocytic processes **(i, j)**. Scale bar: 50 µm.

The quantification of SAs amount showed that, even though they appear in stage I, there is a huge increase in number in the intermediate and advanced stages. It achieves statistically significant differences for I (0.36±0.11 N=30) vs. II (3.47±0.78; N=21) ($p < 0.0001$) and I vs. III (3.63±0.77; N=27) ($p<0.0001$) (Fig. 5b).

The density of SAs inside tumors (number of SA/mm^2 of tumor) shows its peak at stage II (1.10±0.22; N=23). Stage I (0.99±0.33; N=28) and stage III (0.54±0.12; N=31) achieve statistically significant difference ($p=0.0222$) compared to stage II (Fig. 5c).

The mean area of the SAs increases during tumor development, without statistically significant differences. In stage I, the area of SAs is 17.39±4.73 μm^2 (N=8), in the intermediate 29.08±6.99 μm^2 (N=67) while it is 29.94±7.59 μm^2 (N=134) in the advanced stage. Huge aggregates, including many abnormal microvessel profiles, can occasionally be found in the most advanced stage (Fig. 5d).

Discussion

The presence of Nestin+cells has been described in humans and in experimental animal models of glioblastomas (Dahlstrand et al., 1992; Matsuda et al., 2013).

Endogenous generation of gliomas in rats is a well-known and reliable model to study gliomas in different stages (Zook and Simmens, 2005; Bulnes-Sesma et al., 2006). In fact, this model has been previously used to research about many cellular, biological and genetic aspects of gliomas during its development (Zook et al.,

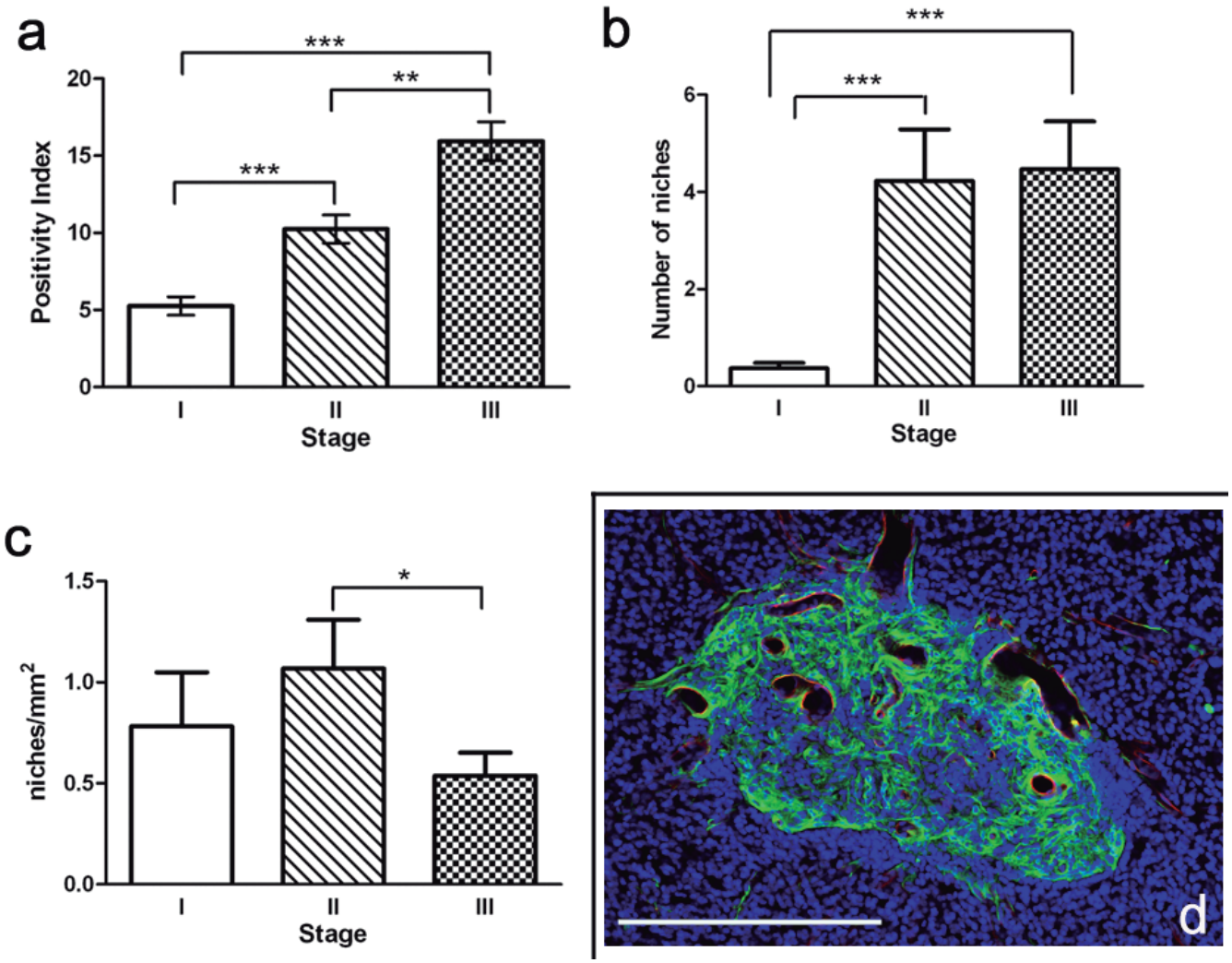

Fig. 5. a. Labelled index of Nestin+cells in the three stages of ENU-gliomas. There is an increase of Nestin+cells corresponding to malignancy, ***p<0.001, **p<0.01. **b.** Mean number of spheroid aggregates in the different stages, almost absent in stage I, and increasing in the second and third stages, ***p<0.001. **c.** Density of aggregates per mm^2 of tumor, the highest density is at stage II *p<0.05. **d.** Double immunofluorescence against Nestin (green) and Glut-1 (red) in an enormous "spheroid aggregate" showing the close interrelation among these structures. Scale bar: 250 μm.

2000; Recht et al., 2003; Jang et al., 2004, 2006; Bulnes et al., 2011). However the present study focused on the distribution of Nestin and CD133 positive cells,, as there is little knowledge about these cells throughout the glioma progression.

In this study, we have observed some Nestin+cells (with a small and round cytoplasm) grouped in spheroid arrangements. These spheroid aggregates would represent an *in vivo* approximation to the tumorspheres. It has been reported that CD133- tumorspheres from human gliomas are capable of forming gliomas in nude rats (Pastrana et al., 2011). This fact could be explained by the heterogeneity of the CSCs and the plasticity theory (Hadjipanayis and Van Meir, 2009), in which the stemness status is not definitive, but rather is linked to the microenvironment. Thus, some CD133-cells could adapt and transform themselves into CD133+cells, capable of generating a tumor.

The results in the present study show that Nestin/CD133+cells are found inside ENU-gliomas, showing specific morphologies depending on different locations. In the hypoxic interior of tumors, cells expressing Nestin and/or CD133 appear located close to tortuous and dilated vessels or in dense groups throughout the tumor forming "spheroid aggregates". According to previous reports, Nestin+cells can be found distributed along vessels (Jang et al., 2004), as CD133+cells forming clusters close to the vascular wall (Arai et al., 2012), as we have ascertained. Other markers have also been reported such as Notch and iNOS (Filatova et al., 2012). These perivascular cells are involved in tumoral angiogenesis. Angiogenesis would be driven mainly by Nestin/CD133+cells placed around aberrant vessels of the tumor. It has been reported that some of these cells, expressing one or both markers and developing in a hypoxic environment, produce HIF-2 alpha inducing the cascade of VEGF (Heddleston et al., 2009). Meanwhile, in the neoangiogenic tumoral border, cells positive for Nestin/CD133 are found to co-express GFAP and VEGF.

Some endothelial cells from glomeruloid vessels showed a light co-localization of CD133 and LEA supporting the hypothesis of cellular transdifferentiation in GBM (Soda et al., 2011). Specifically, it has been hypothesized that CD133+cells can give rise to tumor endothelium (Wang et al., 2010). Co-expression of Nestin and VEGF already in the intermediate stage of ENU-gliomas, when the "angiogenic switch" arises (Bergers and Benjamin, 2003), supports the involvement of these cells in tumoral angiogenesis.

Spheroid aggregates appear in all stages of ENU-gliomas. We have observed that these structures resemble neurospheres in cell morphology, immuno-marker distribution, etc. (Bao et al., 2006). As previously mentioned, the gold standard assay to identify stem cells is the *in vitro* sphere growth (Pastrana et al., 2011). Protocols vary substantially between different assays, but in all of them the absence of growth factors is mandatory to induce the sphere formation. So, stem cells could form spheres *in vitro* in order to protect themselves against adverse conditions such as lack of nutrients. In the same way, Nestin/CD133+cells *in vivo* could form the spheroid aggregates to protect themselves against hypoxia, lack of nutrients or maybe also chemotherapeutics (Rich, 2007; Denysenko et al., 2010). Cells from spheroid aggregates could stimulate cells around them or produce themselve angiogenic factors in order to escape from adverse conditions.

The highest density of aggregates was found in the intermediate tumoral stage. In the most malignant stage the spheroid density is reduced, although the surface occupied by them increases. One possible explanation would be that small aggregates grow and probably come together forming the big ones, being less in number but bigger in size.

Accordingly we also observed that the mean size of spheroid aggregates increased with malignancy. It has been reported that even though the *in vitro* size of tumorspheres varies greatly, between 40-150 μm (Pastrana et al., 2011), it is possible to culture huge neurospheres with 300 or even 400 μm of diameter under certain conditions (Mori et al., 2006); similarly we could observe occasionally some huge aggregates in the most malignant gliomas.

Nestin has been described as a marker of undifferentiated states and degree of malignancy (Singh et al., 2003; Schiffer et al., 2010). Some Nestin+cells having a round and compact morphology were considered as stem-like cells and are located mainly in the spheroid aggregates and in the perivascular region, named "perivascular niche" (Christensen et al., 2008). By contrast, the big cells with cellular prolongations located specially around the tumoral border or surrounding aggregates are more probably reactive astrocytes because they are also positive for GFAP.

It has been previously theorized that perivascular niches could act as a reservoir of undifferentiated cells and could be responsible for the high rate of relapse in malignant gliomas (Christensen et al., 2011). Further research is needed to elucidate the role of spheroid aggregates and to better understand their parallelism to tumorspheres, but they could play a similar role to the those previously described perivascular niches. However, if the spheroid aggregates in the ENU-model were really tumorspheres analogues, this would open up new ways to research the "spheres" behaviour *in vivo*, and the relation with other structures like the tumoral vasculature. Therefore, the ENU-induced tumor model could provide helpful information to aid in understanding the nature of cancer stem cells and their properties. An *in vivo* characterization would be the first step for a proper identification, giving rise to guided therapies against these cells, as they are the ones that lead the tumorigenesis and angiogenesis processes.

The ENU model is useful to provide information about the properties and nature of undifferentiated tumoral cells and their arrangements, making possible the identification of clusters of Nestin and CD133+cells

resembling *in vitro* created tumorspheres. ENU model also is a useful way to design new strategies for *in vivo* identification of cancer stem cells that could lead to specific therapeutic approaches.

Acknowledgements. This study has been partially supported by SAIOTEK (Department of Industry, Government of the Basque Country), GIC IT/794/13 (Basque Government) and UFI 11/32 (University of Basque Country).

References

Adey W.R., Byus C.V., Cain C.D., Jones R.A., Kean C.J., Kuster N., MacMurray A., Stagg R.B. and Zimmerman G. (2000). Spontaneous and nitrosourea-induced primary tumors of the central nervous system in Fischer 344 rats exposed to frequency-modulated microwave fields. Cancer Res. 60, 1857-1863.

Arai H., Ikota H., Sugawara K., Nobusawa S., Hirato J. and Nakazato Y. (2012). Nestin expression in brain tumors: its utility for pathological diagnosis and correlation with the prognosis of high-grade gliomas. Brain Tumor Pathol. 29, 160-167.

Bao S., Wu Q., McLendon R.E., Hao Y., Shi Q., Hjelmeland A.B., Dewhirst M.W., Bigner D.D. and Rich J.N. (2006). Glioma stem cells promote radioresistance by preferential activation of the DNA damage response. Nature 444, 756-760.

Bergers G. and Benjamin L.E. (2003). Tumorigenesis and the angiogenesis switch. Nat. Rev. Cancer 3, 401-410.

Bulnes S. and Lafuente J.V. (2007). VEGF immunopositivity related to malignancy degree, proliferative activity and angiogenesis in ENU-induced gliomas. J. Mol. Neurosci. 33, 163-172.

Bulnes-Sesma S., Ullibarri-Ortiz de Zarate N. and Lafuente-Sanchez J.V. (2006). Tumour induction by ethylnitrosourea in the central nervous system. Rev. Neurol. 43, 733-738.

Bulnes S., Garcia-Blanco A., Bengoetxea H., Ortuzar N., Argandona E.G. and Lafuente J.V. (2011). Glial stem cells and their relationship with tumour angiogenesis process. Rev. Neurol. 52, 743-750.

Christensen K., Schroder H.D. and Kristensen B.W. (2008). CD133 identifies perivascular niches in grade II-IV astrocytomas. J. Neurooncol. 90, 157-170.

Christensen K., Schroder H.D. and Kristensen B.W. (2011). CD133+ niches and single cells in glioblastoma have different phenotypes. J. Neurooncol. 104, 129-143.

Clarke M.F., Dick J.E., Dirks P.B., Eaves C.J., Jamieson C.H., Jones D.L., Visvader J., Weissman I.L. and Wahl G.M. (2006). Cancer stem cells perspectives on current status and future directions: AACR Workshop on cancer stem cells. Cancer Res. 66, 9339-9344.

Dahlstrand J., Collins V.P. and Lendahl U. (1992). Expression of the class VI intermediate filament nestin in human central nervous system tumors. Cancer Res. 52, 5334-5341.

Dell'Albani P. (2008). Stem cell markers in gliomas. Neurochem. Res. 33, 2407-2415.

Denysenko T., Gennero L., Roos M.A., Melcarne A., Juenemann C., Faccani G., Morra I., Cavallo G., Reguzzi S., Pescarmona G. and Ponzetto A. (2010). Glioblastoma cancer stem cells: heterogeneity, microenvironment and related therapeutic strategies. Cell Biochem. Funct. 28, 343-351.

Doblas S., He T., Saunders D., Hoyle J., Smith N., Pye Q., Lerner M., Jensen R.L. and Towner R.A. (2012). *In vivo* characterization of several rodent glioma models by 1H MRS. NMR Biomed. 25, 685-694.

Fan X., Salford L.G. and Widegren B. (2007). Glioma stem cells: evidence and limitation. Semin. Cancer Biol. 17, 214-218.

Filatova A., Acker T. and Garvalov B.K. (2012). The cancer stem cell niche(s): The crosstalk between glioma stem cells and their microenvironment. Biochim. Biophys. Acta 1830, 2496-2508.

Gondo Y., Fukumura R., Murata T. and Makino S. (2010). ENU-based gene-driven mutagenesis in the mouse: a next-generation gene-targeting system. Exp. Anim. 59, 537-548.

Grosse-Gehling P., Fargeas C.A., Dittfeld C., Garbe Y., Alison M.R., Corbeil D. and Kunz-Schughart L.A. (2013). CD133 as a biomarker for putative cancer stem cells in solid tumours: limitations, problems and challenges. J. Pathol. 229, 355-378.

Hadjipanayis C.G. and Van Meir E.G. (2009). Brain cancer propagating cells: biology, genetics and targeted therapies. Trends Mol. Med. 15, 519-530.

Heddleston J.M., Li Z., McLendon R.E., Hjelmeland A.B. and Rich J.N. (2009). The hypoxic microenvironment maintains glioblastoma stem cells and promotes reprogramming towards a cancer stem cell phenotype. Cell Cycle 8, 3274-3284.

Jang T., Litofsky N.S., Smith T.W., Ross A.H. and Recht L.D. (2004). Aberrant nestin expression during ethylnitrosourea-(ENU)-induced neurocarcinogenesis. Neurobiol. Dis. 15, 544-552.

Jang T., Savarese T., Low H.P., Kim S., Vogel H., Lapointe D., Duong T., Litofsky N.S., Weimann J.M., Ross A.H. and Recht L. (2006). Osteopontin expression in intratumoral astrocytes marks tumor progression in gliomas induced by prenatal exposure to N-ethyl-N-nitrosourea. Am. J. Pathol. 168, 1676-1685.

Jensen J.B. and Parmar M. (2006). Strengths and limitations of the neurosphere culture system. Mol. Neurobiol. 34, 153-161.

Kronenberg G., Reuter K., Steiner B., Brandt M.D., Jessberger S., Yamaguchi M. and Kempermann G. (2003). Subpopulations of proliferating cells of the adult hippocampus respond differently to physiologic neurogenic stimuli. J. Comp. Neurol. 467, 455-463.

Matsuda Y., Hagio M. and Ishiwata T. (2013). Nestin: a novel angiogenesis marker and possible target for tumor angiogenesis. World J. Gastroenterol. 19, 42-48.

Messam C.A., Hou J. and Major E.O. (2000). Coexpression of nestin in neural and glial cells in the developing human CNS defined by a human-specific anti-nestin antibody. Exp. Neurol. 161, 585-596.

Mori H., Ninomiya K., Kino-oka M., Shofuda T., Islam M.O., Yamasaki M., Okano H., Taya M. and Kanemura Y. (2006). Effect of neurosphere size on the growth rate of human neural stem/progenitor cells. J. Neurosci. Res. 84, 1682-1691.

Morrison S.J. and Kimble J. (2006). Asymmetric and symmetric stem-cell divisions in development and cancer. Nature 441, 1068-1074.

Pastrana E., Silva-Vargas V. and Doetsch F. (2011). Eyes wide open: a critical review of sphere-formation as an assay for stem cells. Cell Stem Cell. 8, 486-498.

Recht L., Jang T., Savarese T. and Litofsky N.S. (2003). Neural stem cells and neuro-oncology: quo vadis?. J. Cell Biochem. 88, 11-19.

Rich J.N. (2007). Cancer stem cells in radiation resistance. Cancer Res. 67, 8980-8984.

Schiffer D., Annovazzi L., Caldera V. and Mellai M. (2010). On the origin and growth of gliomas. Anticancer Res. 30, 1977-1998.

Singh S.K., Clarke I.D., Terasaki M., Bonn V.E., Hawkins C., Squire J. and Dirks P.B. (2003). Identification of a cancer stem cell in human brain tumors. Cancer Res. 63, 5821-5828.

Singh S.K., Clarke I.D., Hide T. and Dirks P.B. (2004). Cancer stem cells in nervous system tumors. Oncogene 23, 7267-7273.

Soda Y., Marumoto T., Friedmann-Morvinski D., Soda M., Liu F., Michiue H., Pastorino S., Yang M., Hoffman R.M., Kesari S. and Verma I.M. (2011). Transdifferentiation of glioblastoma cells into vascular endothelial cells. Proc. Natl. Acad. Sci. USA 108, 4274-4280.

Wang R., Chadalavada K., Wilshire J., Kowalik U., Hovinga KE., Geber A., Fligelman B., Leversha M., Brennan C. and Tabar V. (2010). Glioblastoma stem-like cells give rise to tumour endothelium. Nature 468, 829-833.

Zook B.C. and Simmens. S.J. (2005). Neurogenic tumors in rats induced by ethylnitrosourea. Exp. Toxicol. Pathol. 57, 7-14.

Zook B.C., Simmens S.J. and Jones R.V. (2000). Evaluation of ENU-induced gliomas in rats: nomenclature, immunochemistry, and malignancy. Toxicol. Pathol. 28, 193-201.

Accepted April 1, 2016